

Modulation of Cell Differentiation, Proliferation, and Tumor Growth by Dihydrobenzyloxypyrimidine Non-Nucleoside Reverse Transcriptase Inhibitors

Gianluca Sbardella,^{*,†} Antonello Mai,^{*,‡} Sara Bartolini,[§] Sabrina Castellano,[†] Roberto Cirilli,[§] Dante Rotili,[‡] Ciro Milite,[†] Marisabella Santoriello,[†] Serena Orlando,^{||} Ilaria Sciamanna,[§] Annalucia Serafino,[⊥] Patrizia Lavia,^{||} and Corrado Spadafora[§]

[†]Dipartimento di Scienze Farmaceutiche e Biomediche, Epigenetic Med Chem Lab, Università degli Studi di Salerno, Via Ponte Don Melillo, I-84084 Fisciano (SA), Italy

[‡]Istituto Pasteur—Fondazione Cenci Bolognetti, Dipartimento di Chimica e Tecnologie del Farmaco, Sapienza Università di Roma, P.le A. Moro 5, I-00185 Rome, Italy

[§]Istituto Superiore di Sanità, Viale Regina Elena 299, I-00161 Rome, Italy

^{||}Istituto di Biologia Molecolare e Patologia, CNR, c/o Sapienza Università di Roma, Via degli Apuli 4, I-00185 Rome, Italy

[⊥]Istituto di Farmacologia Traslazionale, CNR, Via Fosso del Cavaliere 100, 00133, Rome, Italy

Supporting Information

ABSTRACT: A series of 5-alkyl-2-(alkylthio)-6-(1-(2,6-difluorophenyl)propyl)-3,4-dihydropyrimidin-4(3H)-one derivatives (**3a–h**) belonging to the F_2 -DABOs class of non-nucleoside HIV-1 reverse transcriptase inhibitors (NNRTIs) are endowed with a strong antiproliferative effect and induce cytodifferentiation in A375 melanoma cells. Among tested compounds, the most potent is **3g** (SPV122), which also induces apoptosis in a cell-density-dependent manner and antagonizes tumor growth in animal models. All these effects are similar or even more pronounced than those previously reported for other nucleoside or non-nucleoside inhibitors of reverse transcriptase or by functional knockout of the reverse-transcriptase-encoding long interspersed element 1 by RNA interference (RNAi). Taken together with our previously reported results, these data further confirm our idea that cellular alterations induced by NNRTIs are a consequence of the inhibition of the endogenous reverse transcriptase in A375 cells and support the potential of NNRTIs as valuable agents in cancer therapy.

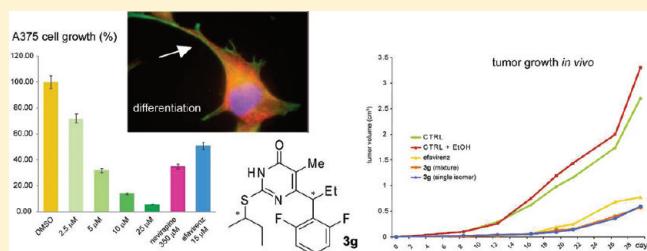
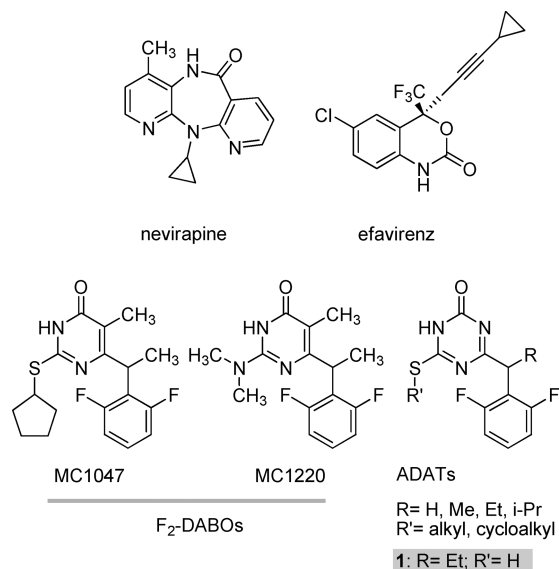


Chart 1



pharmacological inhibition of endogenous RT activity using non-nucleoside inhibitors (NNRTIs), such as nevirapine²¹ and efavirenz²² (Chart 1), or down-regulating RT expression using LINE-1-specific interfering RNAs (siRNAs) causes a significant reduction of cell proliferation, promotes differentiation in tumorigenic cell lines, and strongly antagonizes human tumor progression in murine models.^{23–27} More recently, nucleoside reverse transcriptase inhibitors (NRTIs) have also been reported to suppress LINE-1 retrotransposition activity and to exert antiproliferative effects on tumor cell lines.^{28,29} On the whole, these results suggest that an RT-dependent mechanism operates in transformed cells. Suppressing the RT-dependent mechanism restores control of cell differentiation and proliferation.³⁰ In this context, NNRTIs can be viewed as useful therapeutic tools, able to counteract the loss of differentiation in dedifferentiating pathologies and as antiproliferative drugs in tumor therapy.^{27,31}

Inspired by this evidence, we resolved to investigate the effect on tumor cells of F_2 -DABOs (Chart 1),^{25,26} potent non-nucleoside HIV-1 reverse transcriptase inhibitors developed by our group after a decade of lead optimization studies.^{32–43} We found that two compounds (MC1047 and MC1220) significantly reduced cell proliferation and facilitated the morphological differentiation of human melanoma A375 cells.²⁵ We next decided to replace the substituted C5 of the pyrimidine ring with a nitrogen atom, as triazine-containing compounds are reported to induce the down-regulation of telomerase (hTERT), another human reverse transcriptase.⁴⁴ Although the resulting 6-alkylthio-4-[1-(2,6-difluorophenyl)alkyl]-1*H*-[1,3,5]triazin-2-one (ADAT, Chart 1) derivatives were generally less active than F_2 -S-DABOs, the effects that they induced in the A375 melanoma cell line did closely resemble those previously observed with either NNRTIs or RNA interference (RNAi)-mediated silencing of RT-encoding LINE-1 elements. Moreover, cell growth inhibition by either established NNRTIs or ADATs was reversible and not inherited as a permanent change through cell division. This suggests that the phenotypic variations induced by RT inhibition in cultured cells are of an epigenetic nature and are independent of insertional mutagenic events.²⁶ Surprisingly, we noticed that compound **1** (Chart 1), characterized by a 6-thioxotriazin-2-one

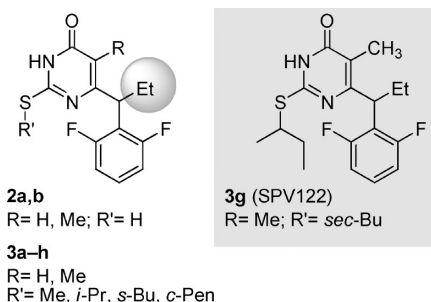
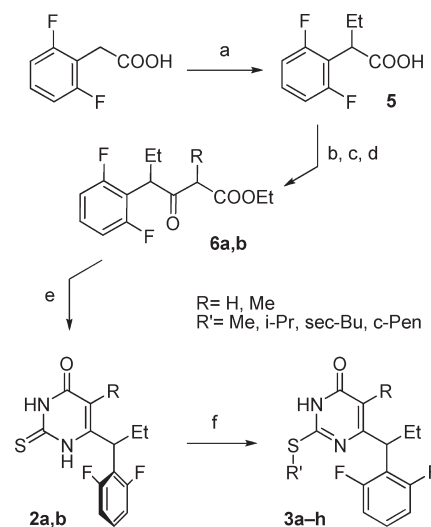


Figure 1

Scheme 1^a

^a Reagents and conditions: (a) *n*-BuLi, EtI, THF, $-10\text{ }^\circ\text{C}$; (b) CDI, CH_3CN ; (c) potassium ethylmalonate or potassium ethyl-2-methylmalonate, MgCl_2 , TEA, CH_3CN ; (d) 12% HCl; (e) thiourea, Na, EtOH, reflux; (f) alkyl iodide, K_2CO_3 , DMF.

structure and by the presence of an ethyl substituent at the linker position, though not affecting cell proliferation, showed a strong cytodifferentiating effect and a marked up-regulation of the E-cadherin (*e-cad*) gene; in contrast, the corresponding linker-unsubstituted analogue was found to be substantially inactive in the same assay.²⁶ This evidence suggested a crucial role of the ethyl substituent in this position.

Here we report on the activity of a series of pyrimidinones derivatives designed on the basis of structure–activity relationships resulting from both F_2 -DABOs and ADATs series. Among them we identified **3g** (SPV122, Figure 1), a compound that significantly inhibits cell proliferation and induces differentiation in A375 melanoma cells and is able to inhibit tumor growth in nude mice.

CHEMISTRY

Derivatives **2** and **3** were prepared, following a straightforward procedure previously described by us, starting from 2-(2,6-difluorophenyl)butanoic acid (compound **5**),^{26,38} promptly obtained by alkylation of (2,6-difluoro)phenylacetic acid with ethyl iodide in the presence of *n*-butyl lithium in anhydrous THF (Scheme 1). The imidazolidine obtained from the acid **5** by

Table 1. Inhibition of Proliferation by Compounds **2a,b** and **3a–h**^a

compd	R	R'	cell growth (% at 25 μM) ^b
control			100
2a	H	H	100
3a	H	Me	13
3b	H	<i>i</i> -Pr	19
3c	H	<i>s</i> -Bu	13
3d	H	<i>c</i> -Pen	22
2b	Me	H	76
3e	Me	Me	40
3f	Me	<i>i</i> -Pr	12
3g	Me	<i>s</i> -Bu	5
3h	Me	<i>c</i> -Pen	5
NEV (350 μM)			35
EFV (15 μM) ^c			51

^a Cell growth in human A375 melanoma cultures treated with DMSO (control), test compounds, nevirapine (NEV), and efavirenz (EFV).

^b Cells were treated for 96 h, then harvested and counted. Counted cells are expressed as the % of controls, taken as 100. Values represent pooled data from three experiments. ^c In the condition of the assay, this is the highest testable concentration of efavirenz before the occurrence of cytotoxic effects.

treatment with *N,N'*-carbonyldiimidazole (CDI) was then reacted with potassium ethylmalonate or potassium ethyl-2-methylmalonate in the presence of the magnesium dichloride/triethylamine system to yield, after decarboxylation with 12% hydrochloric acid, the ethyl 4-(2,6-difluorophenyl)-3-oxohexanoates **6a,b**.^{38,43} Condensation of these β -oxoesters with thiourea in the presence of sodium ethoxide gave the intermediate 6-(1-(2,6-difluorophenyl)propyl)-2-thioxo-2,3-dihydropyrimidin-4(1*H*)-one **2a** and 6-(1-(2,6-difluorophenyl)propyl)-5-methyl-2-thioxo-2,3-dihydropyrimidin-4(1*H*)-one **2b**,⁴⁵ respectively, which were finally *S*-alkylated in dry DMF with the proper alkyl halide in the presence of potassium carbonate to yield the corresponding compounds **3a–h**.

RESULTS

Compounds **2a,b** and **3a–h** were tested (25 μM in DMSO solution) on the human A375 cell line, derived from metastatic malignant melanoma (ATCC CRL-1619), previously characterized in depth for being sensitive to both siRNA-mediated silencing of RT-encoding LINE-1 elements and to NNRTI-mediated (nevirapine and efavirenz) RT inhibition.^{24,46} Nevirapine and efavirenz were used as reference drugs (Table 1). With the exception of the two *S*-unsubstituted compounds **2a** and **2b**, all tested derivatives exhibited a strong antiproliferative effect, being more effective than references at concentrations 14-fold lower than that employed for nevirapine.³⁸ Moreover, derivatives **3a–h** are more active than the corresponding methyl-substituted

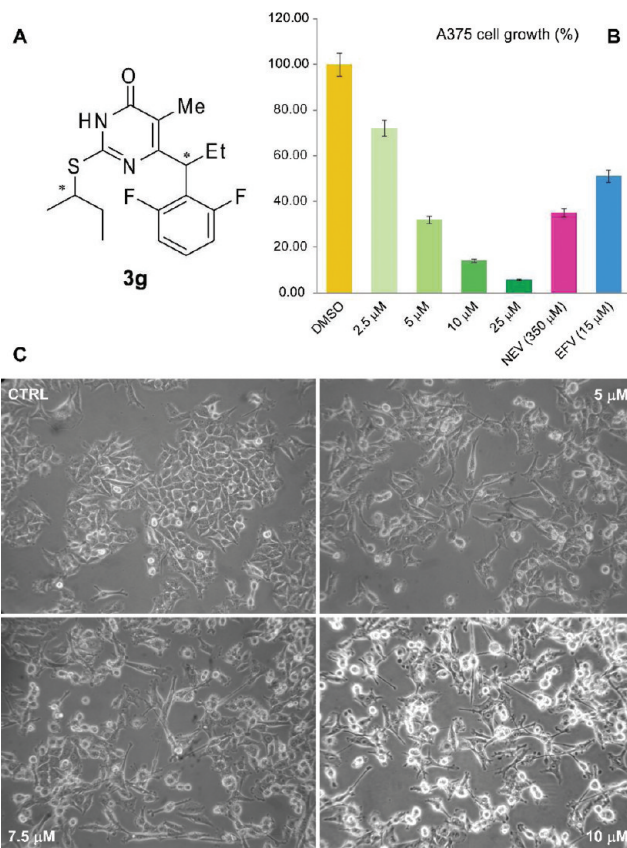


Figure 2. Effects of **3g** (A) on the human melanoma A375 cell line. (B) Cell growth in human A375 melanoma cultures treated with DMSO (control), **3g** at increasing concentrations (2.5, 5, 10, 25 μM), nevirapine (NEV, 350 μM), and efavirenz (EFV, 15 μM). Cells were harvested and counted after 96 h. Counted cells are expressed as the % of controls, taken as 100. Values represent pooled data from three experiments. (C) Morphological differentiation of A375 melanoma cells in the presence of DMSO (control) and **3g** (5, 7.5, and 10 μM) under phase-contrast microscopy.

analogues. For example, when A375 cells were treated with derivative **3h** at 25 μM , a very low growth rate (5%) was observed. Under the same conditions, cells treated with MC1047, the methyl substituted analogue of **3h**, displayed a significantly higher growth rate (72%).²⁵ This result substantiates the importance of the ethyl substituent on the methylene connecting phenyl with triazine or, in this case, pyrimidine ring (linker position). In general, the antiproliferative capability of the compounds is related to the size of the substituent on the sulfur atom at the C2 position of the pyrimidine ring. This effect is further increased by the insertion of a methyl group at the C5 position (compare, for example, the activities of compounds **3b**, **3c**, and **3d** with those of **3f**, **3g**, and **3h**, respectively).

The derivative **3g** (SPV122) (Figure 2A) showed the most powerful antiproliferative effect. To characterize this effect in more depth, we carried in vitro growth assays out by exposing A375 cultures to increasing doses of the compound. As shown in Figure 2B, the antiproliferative effect exerted by **3g** was highly dose-dependent and markedly stronger than that induced by efavirenz at approximately equivalent dosage. In addition, **3g**, even in low concentrations (i.e., 5, 7.5, and 10 μM), induced remarkable morphological changes in A375 cells compared to DMSO-treated controls (Figure 2C); dendritic-like extensions

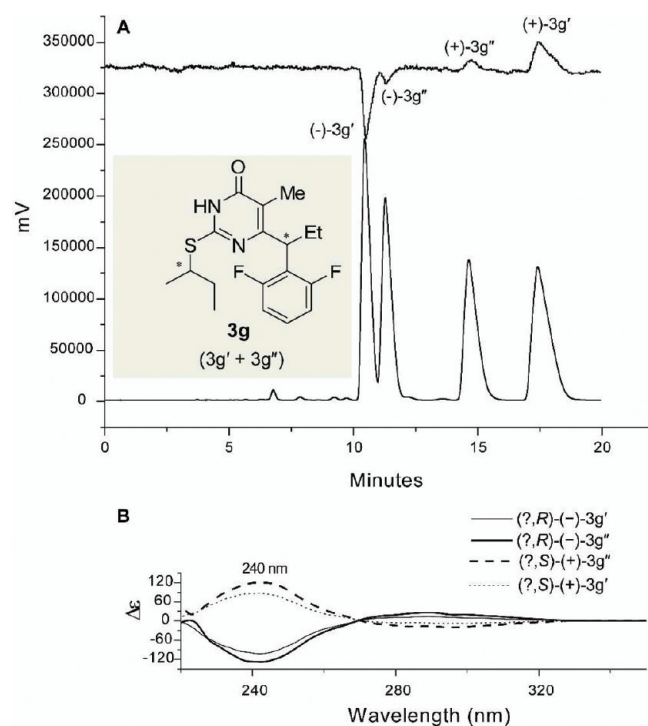


Figure 3. HPLC separation of the four stereoisomers of **3g**.⁴⁸ (A) Polarimetric (365 nm) (top) and UV (330 nm) (bottom) chromatograms of **3g**: column, Chiralpak IA (250 mm × 10 mm i.d.); eluent MTBE–EtOAc (75:25, v/v); flow rate of 1 mL/min; column temperature of 25 °C. (B) CD spectra of the stereoisomers of **3g** in ethanol at 25 °C.

were induced and adhesion increased, strongly suggesting that a differentiation process was activated.^{24–26,47}

Separation of **3g Stereoisomers.** Compound **3g** has two stereogenic centers; therefore, the biological effects ascribed to this compound are in fact the resultant of a mixture of four stereoisomers. In order to assess the biological effect of each single stereoisomer, we decided to separate them using HPLC in a single run on the immobilized-type Chiralpak IA chiral stationary phase (CSP) using ethyl acetate based eluents.⁴⁸ Different from closely related compounds,⁴⁹ in this case the assignment of absolute configuration by X-ray diffraction analysis was not possible because of unfavorable physical properties of the isolated stereoisomers and difficulty in obtaining crystalline derivatives. By analysis of the sign of optical rotation and relative peak areas (Figure 3), it was possible to identify the first and the fourth eluted stereoisomer as belonging to the same enantiomeric pair (compound **3g'**) and the second and third one to the diastereomeric pair of enantiomers (compound **3g''**). Moreover, the analogy between the circular dichroism (CD) profiles of **3g** and its dichlorophenyl analogue⁴⁹ permitted assignment of the (R) absolute configuration to the stereogenic center adjacent to the 2,6-difluorophenyl moiety of (–)-**3g'** and (–)-**3g''**. The configurational assignment about the stereogenic center of *sec*-butylthio group of **3g** still remains an unsolved question. After separation, the four stereoisomers were individually tested in biological experiments, in comparison with the **3g** mixture (hereafter simply referred to as **3g**) and nevirapine.

Inhibition of Cell Proliferation. In the first set of experiments, stereoisomers were tested in increasing doses (5, 10, and 20 μM) for their antiproliferative efficacy in comparison to

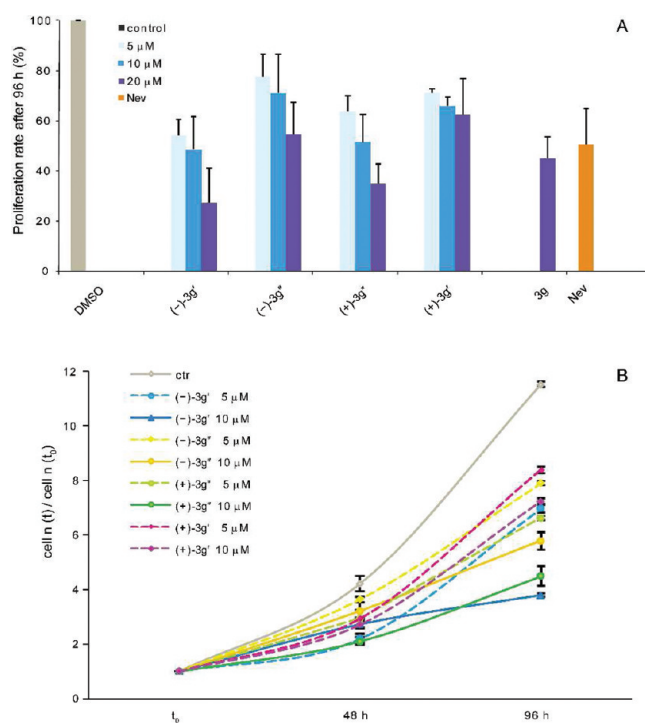


Figure 4. Stereoisomers **3g** inhibit proliferation of A375 melanoma cells in a dose-dependent (A) and time-dependent (B) manner. (A) The histograms represent the extent of cell proliferation in A375 cell cultures exposed to the indicated treatments for 96 h (mean values and SD from four independent experiments). The ratio of proliferating cells after treatment/seeded cells is expressed relative to that measured in DMSO-exposed control samples, taken as 100%. For comparison, 20 μM **3g** and 350 μM nevirapine were used. (B) A375 melanoma cell cultures were exposed to **3g** stereoisomers (5 or 10 μM) or to DMSO only (control), and cells were counted at the indicated times (mean values and SD from three experiments).

unfractionated **3g** (20 μM), nevirapine (NEV, 350 μM), or DMSO alone for control. The results in Figure 4 show that all four stereoisomers inhibited proliferation of A375 melanoma cells compared to solvent-treated control samples. The stereoisomers exhibited different individual effectiveness in terms of their growth inhibitory properties: (–)-**3g'** and (+)-**3g''** were identified as the most effective of the four isolated stereoisomers and in comparison to **3g**. The repressive effect is both dose-dependent, with 20 μM yielding the most powerful antiproliferative effect (70–80% suppression of the proliferation, Figure 4A), and time-dependent (with a most pronounced effect after 96 h compared to 48 h for all compounds, Figure 4B) for all stereoisomers. It is noteworthy that repression of proliferation by the most effective stereoisomers at 20 μM was consistently higher than observed with 350 μM nevirapine, which leaves a cycling subpopulation representing almost 50% of the original culture after 96 h of treatment.

Induction of Apoptosis. In preliminary experiments we found that **3g** induces apoptotic cell death in a dose-dependent manner, as shown by combined staining with propidium iodide (PI) to reveal permeable necrotic cells, 4',6-diamidino-2-phenylindole lactate (DAPI) to visualize apoptotic nuclei, and 3,3-dihexyloxycarbocyanine [DiOC6(3)]^{24,50} to monitor the loss of mitochondrial transmembrane potential (Supporting Information, Figure S1), similar to previously analyzed NNRTIs.^{23–26}

A fraction of necrotic cells only became apparent with the highest tested dose (25 μM).

We next investigated the ability of the single separated stereoisomers to induce apoptotic cell death. A375 cells were seeded at low density (100 000 cells per 25 mm^2 flask), cultured for 96 h in the presence of compounds (20 μM), then harvested and subjected to biparametric fluorescence-activated cell sorting (FACS) analysis (the nuclear DNA profiles were revealed by PI incorporation and the cell granular density by side scatter analysis, SSC). This revealed a very low induction of apoptosis. When cells were seeded at a higher density (i.e., 300 000 cells per 25 mm^2 flask), however, a significant induction of apoptosis was recorded, especially with (–)-**3g'** and, even more evidently, with (+)-**3g'** (Figure 5). In contrast, nevirapine failed to induce significant apoptosis in either condition. To distinguish apoptotic cell death from necrosis, the results were confirmed in bipara-

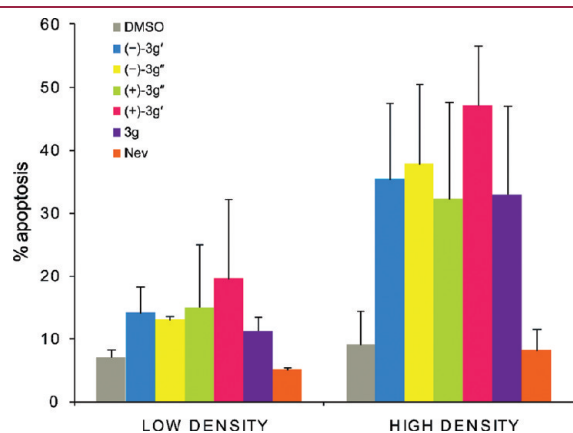
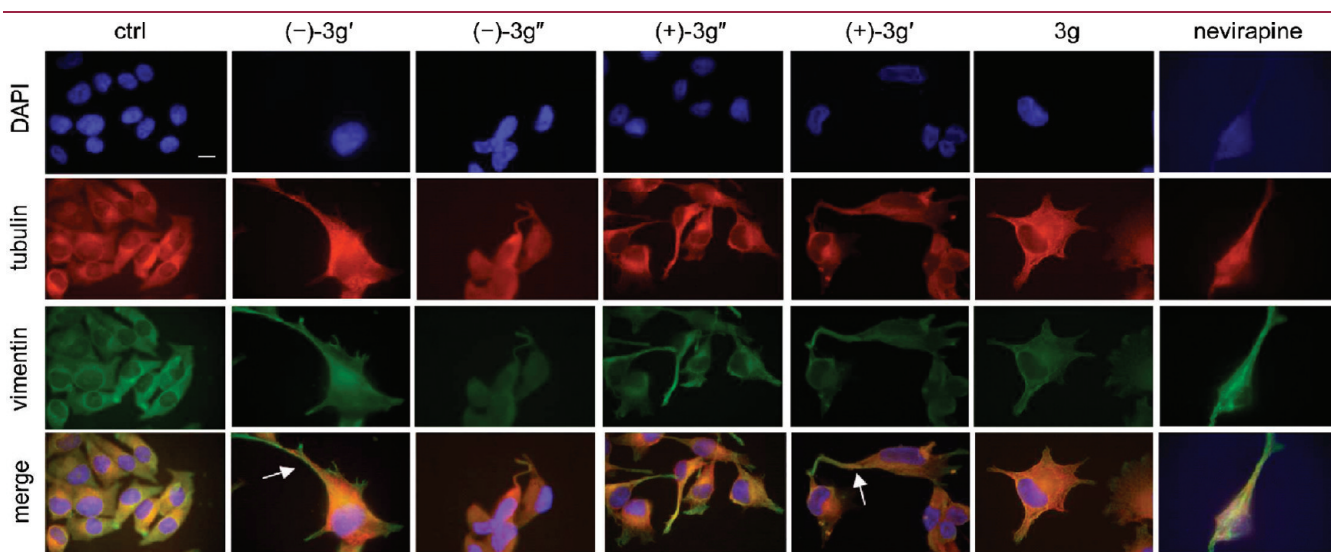


Figure 5. Density-dependent effect induction of apoptosis by **3g** stereoisomers. The histograms represent the mean and SD values (three experiments) of the apoptotic cell population, revealed by FACS analysis in A375 melanoma cell cultures plated at low and high density.

metric FACS analysis of the nuclear DNA content (PI) combined with annexin V (which detects phosphatidylserine residues translocated from the inner to the outer cell membrane in early apoptotic stages) and in indirect immunofluorescence (IF) analysis of cells expressing active caspase-3 (data not shown). Together these assays indicate that the **3g** mixture, as well as each single stereoisomer, induces a specific apoptotic response in A375 melanoma cells in a cell-density-dependent manner.

Morphological Differentiation. The observation (under bright-field microscopy) of A375 cells cultured in the presence of the stereoisomers, particularly with (–)-**3g'** and (+)-**3g'**, indicated clear signs of morphological differentiation, with the appearance of dendritic-like extensions (Figure 2C and Figure S2, Supporting Information). To refine this analysis, we used antibodies to tubulin and vimentin intermediate filament in IF assays. As shown in Figure 6, after 96 h of exposure a clear reorganization of microtubules and of the vimentin intermediate filament network was revealed, with an evident induction of elongated extensions. Scoring of cells that underwent these morphological changes (representative examples are shown in Figure S3A, Supporting Information) indicated that all four isomers induce differentiation more effectively than nevirapine (Figure S3B), albeit to varying extent: both enantiomers (–)-**3g'** and (+)-**3g'** were particularly effective, whereas surprisingly (+)-**3g''**, which had a strong antiproliferative effect, was a somewhat weaker inducer of differentiation.

Compound **3g Antagonizes Tumor Progression.** Given that **3g** can suppress proliferation and induce differentiation in transformed cells, we next asked whether it also affects tumor growth in vivo. To that aim, A375 cells were inoculated subcutaneously in the limb of athymic nude mice. Animals were then subjected to treatment with either **3g** or isomer (–)-**3g'**, endowed with the strongest antiproliferative activity (vide supra); efavirenz was used as the reference drug because it had shown higher in vivo effectiveness than nevirapine in previous assays.²⁴



A375 cells cultured for 96h in DMSO, NEV, **3g** or each single stereoisomer (100 \times)

Figure 6. Reorganization of the cytoskeleton and appearance of dendritic-like extensions in A375 human melanoma cells after treatment with **3g** stereoisomers. A375 cell samples were cultured for 96 h as indicated, then processed for IF to tubulin (red) and vimentin intermediate filament (green). Nuclei are stained with DAPI (blue). Arrows indicate the appearance of dendritic-like extensions, absent in control (DMSO-treated) cultures (100 \times objective).

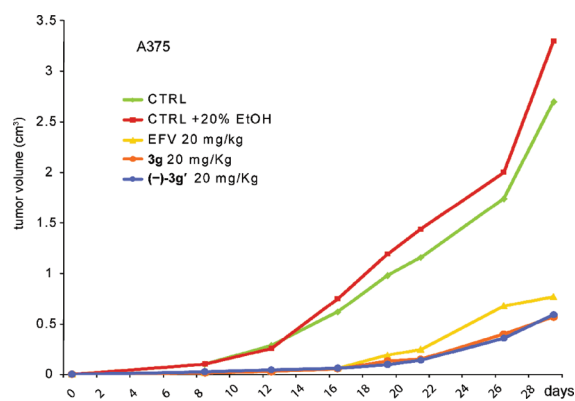


Figure 7. Treatment with **3g** antagonizes human tumor growth in nude mice. The growth of tumors formed by A375 melanoma cells was monitored in nude mice untreated or treated as indicated. Curves show the mean value of tumor size in groups of five animals.

Previous dose–response experiments with efavirenz (testing 4–40 mg drug/kg animal body weight) indicated that 20 mg/kg was the optimal dose for inhibition of progression of xenografted tumors in nude mice.²⁴ All compounds were therefore used at that dose. The growth of A375 melanoma-derived tumor xenografts was monitored, and Figure 7 shows the recorded curves in nude mice untreated or treated with solvent (20% ethanol), efavirenz, **3g**, and isomer (–)-**3g'**. Tumor growth was markedly reduced in both **3g**- and (–)-**3g'**-treated animals compared to untreated controls (Figure 7). Remarkably, the inhibitory efficacy of the latter was comparable or higher than that of efavirenz. A slight enhancement of tumor growth was observed in solvent-treated compared to untreated control animals (Figure 7, green and red curves, respectively).

CONCLUSIONS

A growing body of evidence now indicates that high levels of endogenous RT activity are typically associated with transformed/tumorigenic phenotypes of mammalian cells. In addition, the inhibition of LINE-1-encoded RT by either nucleosidic or non-nucleosidic inhibitors has been proposed as a novel promising approach in cancer therapy.^{18,23–29,31,51–58}

In this work, we report that ethyl-substituted derivatives **3a–h**, belonging to the F_2 -DABOs class of non-nucleoside HIV-1 reverse transcriptase inhibitors, are endowed with a strong antiproliferative effect on A375 melanoma cells. The importance of the ethyl substituent on the methylene connecting phenyl with the pyrimidine ring (linker position) is further substantiated by the fact that, even when lacking any substitution on the sulfur atom, derivatives bearing an ethyl group at linker position were able to induce differentiation of human A375 cells (see, for example, Supporting Information, Figure S4), associated with up-regulation of the *e-cad* gene (not shown). Particularly strong effects in suppression of cell proliferation and induction of differentiation were induced by compound **3g** (SPV122). Those effects resembled those observed when treating A375 cells with NNRTIs^{23–26} or after RNA interference (RNAi)-mediated silencing of the RT-encoding LINE-1 elements.^{24,46} The effects of these treatments, as well as those presently reported for **3g** and its stereoisomers, are induced quite rapidly (within a few days), supporting the conclusion that all tested molecules share a common target in A375 cells. This is distinctive of molecules

inhibiting non-telomerase activities, as the antiproliferative effect observed after chemical⁵⁹ or genetic⁶⁰ inhibition of the telomerase-associated RT requires several months of continuous exposure to display antiproliferative effects, consistent with a progressive mode of action at telomeres.

Compound **3g** induces apoptosis in a manner that is dependent on the initial cell density, and it antagonizes tumor growth in animal models. These effects are similar or more pronounced than those previously reported for other nucleoside or non-nucleoside inhibitors of reverse transcriptase (abacavir, nevirapine, efavirenz, F_2 -DABOs, ADATs). Our results also reveal a functional specificity in the activity of the single stereoisomers separated from the **3g** mixture: (–)-**3g'** is the best inducer of differentiation, the most effective repressor of proliferation, and a good inducer of apoptosis in dense cell cultures; (+)-**3g''** is nearly as effective as (–)-**3g'** in repressing proliferation, but it is less active as a differentiation-inducing agent; (+)-**3g'** has little activity in repressing proliferation, but nevertheless, it is a good inducer of morphological differentiation and apoptosis. This finding may have interesting possible implications. The stereoisomers may differentially inhibit the bulk of the endogenous cellular RT, with the RT “core” activity being fully blocked by (–)-**3g'**, while residual proapoptotic and differentiating activities would be only partially affected by stereoisomers of different structure. Not mutually exclusive, the stereoisomers may differentially prevent the interaction of the cellular RT with distinct target RNAs and thus differentially affect downstream cellular pathways. No selective antibodies that would discriminate differentially active RT subpopulations are currently available to test these alternatives, but the identification of distinctive functional spectra for individual **3g** stereoisomers can provide promising tools to unravel RT-dependent targets in cancer cells in prospective work.

Taken together, the data indicate a strong antiproliferative and antitumor potential of SPV compounds. Furthermore, they provide further support to the notion, emerging from previous work with NNRTIs, that changes in the tumorigenic phenotypes of A375 cells can arise in consequence of the inhibition of the endogenous RT. These results have important implications for cancer therapy and help to identify activities orchestrated by the endogenous RT at a crucial crossroad between cell proliferation, differentiation, and apoptosis.

EXPERIMENTAL SECTION

Chemistry. All chemicals were purchased from Aldrich Chimica (Milan, Italy) or from Alfa Aesar GmbH (Karlsruhe, Germany) and were of the highest purity. All solvents were reagent grade and, when necessary, were purified and dried by standard methods. All reactions requiring anhydrous conditions were conducted under a positive atmosphere of nitrogen in oven-dried glassware. Standard syringe techniques were used for anhydrous addition of liquids. Reactions were routinely monitored by TLC performed on aluminum-backed silica gel plates (Merck DC, Alufolien Kieselgel 60 F254) with spots visualized by UV light ($\lambda = 254, 365$ nm) or using a $KMnO_4$ alkaline solution. Solvents were removed using a rotary evaporator operating at a reduced pressure of ~ 10 Torr. Organic solutions were dried over anhydrous Na_2SO_4 . Chromatographic separations were performed on silica gel (silica gel 60, 0.015–0.040 mm; Merck DC) columns. Melting points were determined on a Stuart SMP30 melting point apparatus in open capillary tubes and are uncorrected. 1H NMR spectra were recorded at 300 MHz on a Bruker Avance 300 spectrometer. Chemical shifts are reported in δ

(ppm) relative to the internal reference tetramethylsilane (TMS). Mass spectra were recorded on a Finnigan LCQ DECA TermoQuest (San Jose, CA, U.S.) mass spectrometer in electrospray positive and negative ionization modes (ESI-MS). Purity of tested compounds was established by combustion analysis, confirming a purity $\geq 95\%$. Elemental analyses (C, H, N) were performed on a Perkin-Elmer 2400 CHN elemental analyzer at the Laboratory of Microanalysis of the Department of Chemistry and Biology, University of Salerno (Italy); the analytical results were within $\pm 0.4\%$ of the theoretical values. When the elemental analysis is not included, compounds were used in the next step without further purification.

Ethyl 4-(2,6-difluoro)phenyl-3-oxohexanoates **6a**^{26,38} and **6b**⁴³ as well as the corresponding 6-(1-(2,6-difluorophenyl)propyl)-2-thioxo-2,3-dihydropyrimidin-4(1H)-one **2a**³⁸ and 6-(1-(2,6-difluorophenyl)propyl)-5-methyl-2-thioxo-2,3-dihydropyrimidin-4(1H)-one **2b**⁴⁵ were prepared as previously described.

6-(1-(2,6-Difluorophenyl)propyl)-2-(methylthio)pyrimidin-4(3H)-one (3a). A mixture of 6-(1-(2,6-difluorophenyl)propyl)-2-thioxo-2,3-dihydropyrimidin-4(1H)-one (**2a**, 1.00 g, 3.54 mmol), iodomethane (245 μ L, 3.89 mmol), potassium carbonate (490 mg, 3.54 mmol), and 2.00 mL of anhydrous *N,N*-dimethylformamide was stirred at room temperature under N_2 atmosphere for 3 h. After completion (TLC: silica gel/*n*-hexane/EtOAc/MeOH 12:3:1), the mixture was diluted with water (20 mL) and extracted with ethyl acetate (3 \times 40 mL). The organic layers were collected, washed with brine (3 \times 50 mL), dried, and evaporated to furnish a solid residue, which was purified by silica gel chromatography (*n*-hexane/EtOAc/MeOH 12:3:1) to yield compound **3a** (75%) as a white solid. Mp 150–151 °C (acetonitrile). ¹H NMR (300 MHz, CDCl₃) δ 0.88–0.93 (t, *J* = 7.4 Hz, 3H, CHCH₂CH₃), 1.97–2.07 (m, 1H, CHCHH_ACH₃),⁶¹ 2.24–2.31 (m, 1H, CHCHH_BCH₃), 2.46 (s, 3H, SCH₃), 4.11–4.16 (m, 1H, CHCH₂CH₃), 6.11 (s, 1H, C-5 H), 6.81–6.87 (m, 2H, C_{3,5}-H Ar), 7.15–7.21 (m, 1H, C₄-H Ar), 11.71 (bs, 1H, NH exchangeable with D₂O). ESI-MS *m/z*: 297 (M + H)⁺. Anal. (C₁₄H₁₄F₂N₂OS) C, H, N.

6-(1-(2,6-Difluorophenyl)propyl)-2-(isopropylthio)pyrimidin-4(3H)-one (3b)³⁸. Title compound **3b** was obtained as a white solid (60%) starting from **2a** (1.00 g, 3.54 mmol) and 2-iodopropane (400 μ L, 3.89 mmol) according to the same procedure used for **3a**. Mp 148–150 °C (acetonitrile). ¹H NMR (300 MHz, CDCl₃) δ 0.88–0.99 (t, *J* = 7.4 Hz, 3H, CHCH₂CH₃), 1.24–1.26 (d, *J* = 6.8 Hz, 3H, CHCH₃), 1.32–1.34 (d, *J* = 6.8 Hz, 3H, CHCH₃), 2.00–2.11 (m, 1H, CHCHH_ACH₃), 2.21–2.35 (m, 1H, CHCHH_BCH₃), 3.81–3.97 (s, 1H, CH), 4.14–4.19 (m, 1H, CHCH₂CH₃), 6.18 (s, 1H, C-5 H), 6.81–6.87 (m, 2H, C_{3,5}-H Ar), 7.15–7.21 (m, 1H, C₄-H Ar), 11.97 (bs, 1H, NH exchangeable with D₂O). ESI-MS *m/z*: 325 (M + H)⁺. Anal. (C₁₆H₁₈F₂N₂OS) C, H, N.

2-(sec-Butylthio)-6-(1-(2,6-difluorophenyl)propyl)pyrimidin-4(3H)-one (3c). Title compound **3c** was obtained as a white solid mixture of stereoisomers (60%) starting from **2a** (1.00 g, 3.54 mmol) and 2-iodobutane (450 μ L, 3.89 mmol) according to the same procedure used for **3a**. Mp 108–109 °C (acetonitrile). ¹H NMR (300 MHz, CDCl₃) δ 0.85–0.98 (m, 6H, ArCHCH₂CH₃ + SCHCH₂CH₃, overlapped signals), 1.21–1.23, 1.30–1.32 (2 d, 3H, SCHCH₃ first enantiomeric pair + SCHCH₃ second enantiomeric pair), 1.48–1.72 (m, 2H, SCHCH₂), 2.00–2.10 (m, 1H, CHCHH_ACH₃), 2.24–2.34 (m, 1H, CHCHH_BCH₃), 3.70–3.79 (m, 1H, SCH), 4.10–4.15 (m, 1H, CHCH₂CH₃), 6.14 (s, 1H, C-5 H), 6.81–6.86 (m, 2H, C_{3,5}-H Ar), 7.12–7.22 (m, 1H, C₄-H Ar), 9.86 (bs, 1H, NH exchangeable with D₂O). ESI-MS *m/z*: 339 (M + H)⁺. Anal. (C₁₇H₂₀F₂N₂OS) C, H, N.

2-(Cyclopentylthio)-6-(1-(2,6-difluorophenyl)propyl)pyrimidin-4(3H)-one (3d)³⁸. Title compound **3d** was obtained as a white solid (60%) starting from **2a** (1.00 g, 3.54 mmol) and bromocyclopentane (450 μ L, 3.89 mmol) according to the same procedure used for **3a**. Mp 143–144 °C (acetonitrile). ¹H NMR (300 MHz, CDCl₃) δ

0.89–0.94 (t, *J* = 7.4 Hz, 3H, CHCH₂CH₃), 1.55–1.67 (m, 6H, C_{3,4}-H₂ + C_{2,5}-H cyclopentane, overlapped signals), 1.89–1.93 (m, 1H, CHCHH_ACH₃), 2.02–2.10 (m, 2H, C_{2,5}-H cyclopentane), 2.24–2.28 (m, 1H, CHCHH_BCH₃), 3.86–3.90 (m, 1H, SCH), 4.12–4.15 (m, 1H, CHCH₂CH₃), 6.14 (s, 1H, C-5 H), 6.81–6.87 (m, 2H, C_{3,5}-H Ar), 7.15–7.21 (m, 1H, C₄-H Ar), 12.74 (bs, 1H, NH exchangeable with D₂O). ESI-MS *m/z*: 351 (M + H)⁺. Anal. (C₁₈H₂₀F₂N₂OS) C, H, N.

6-(1-(2,6-Difluorophenyl)propyl)-5-methyl-2-(methylthio)pyrimidin-4(3H)-one (3e). A mixture of 6-(1-(2,6-difluorophenyl)propyl)-5-methyl-2-thioxo-2,3-dihydropyrimidin-4(1H)-one (**2b**, 1.00 g, 3.37 mmol), iodomethane (235 μ L, 3.71 mmol), potassium carbonate (466 mg, 3.37 mmol), and 2.00 mL of anhydrous *N,N*-dimethylformamide was stirred at room temperature under N_2 atmosphere for 3 h. After completion (TLC: silica gel/*n*-hexane/EtOAc/MeOH 12:3:1), the mixture was diluted with water (20 mL) and extracted with ethyl acetate (3 \times 40 mL). The organic layers were collected, washed with brine (3 \times 50 mL), dried, and evaporated to furnish a solid residue, which was purified by silica gel chromatography (*n*-hexane/EtOAc/MeOH 12:3:1) to yield compound **3e** (60%) as a white solid. Mp 183–185 °C (benzene/cyclohexane). ¹H NMR (300 MHz, CDCl₃) δ 0.90–0.97 (t, *J* = 7.1 Hz, 3H, CHCH₂CH₃), 2.04–2.29 (m, 2H, CHCHH_ACH₃ + CHCHH_BCH₃, overlapped signals), 2.05 (s, 3H, C-5 CH₃), 2.55 (s, 3H, SCH₃), 4.37–4.48 (m, 1H, CHCH₂CH₃), 6.80–6.86 (m, 2H, C_{3,5}-H Ar), 7.13–7.20 (m, 1H, C₄-H Ar), 11.68 (bs, 1H, NH exchangeable with D₂O). ESI-MS *m/z*: 311 (M + H)⁺. Anal. (C₁₅H₁₆F₂N₂OS) C, H, N.

6-(1-(2,6-Difluorophenyl)propyl)-2-(isopropylthio)-5-methylpyrimidin-4(3H)-one (3f). Title compound **3f** was obtained as a white solid (60%) starting from **2b** (1.00 g, 3.37 mmol) and 2-iodopropane (370 μ L, 3.71 mmol) according to the same procedure used for **3e**. Mp 162–163 °C (benzene/cyclohexane). ¹H NMR (300 MHz, CDCl₃) δ 0.92–0.97 (t, *J* = 7.2 Hz, 3H, CHCH₂CH₃), 1.28–1.30 (d, *J* = 6.8 Hz, 3H, CHCH₃), 1.41–1.43 (d, *J* = 6.8 Hz, 3H, CHCH₃), 2.04 (s, 3H, C-5 CH₃), 2.16–2.25 (m, 2H, CHCHH_ACH₃ + CHCHH_BCH₃, overlapped signals), 3.94–4.03 (s, 1H, CH), 4.33–4.44 (m, 1H, CHCH₂CH₃), 6.79–6.85 (m, 2H, C_{3,5}-H Ar), 7.11–7.18 (m, 1H, C₄-H Ar), 11.97 (bs, 1H, NH exchangeable with D₂O). ESI-MS *m/z*: 339 (M + H)⁺. Anal. (C₁₇H₂₀F₂N₂OS) C, H, N.

2-(sec-Butylthio)-6-(1-(2,6-difluorophenyl)propyl)-5-methylpyrimidin-4(3H)-one (3g). Title compound **3g** was obtained (60%) as a white solid mixture of stereoisomers (NMR; see Supporting Information, Figures S5 and S6) starting from **2b** (1.00 g, 3.37 mmol) and 2-iodobutane (430 μ L, 3.71 mmol) according to the same procedure used for **3e**. Mp 137–138 °C (benzene/cyclohexane). ¹H NMR (300 MHz, CDCl₃) δ 0.90–1.06 (m, 6H, ArCHCH₂CH₃ + SCHCH₂CH₃, overlapped signals), 1.24–1.27, 1.40–1.42 (2 d, 3H, SCHCH₃ first enantiomeric pair + SCHCH₃ second enantiomeric pair), 1.55–1.81 (m, 2H, SCHCH₂), 2.03 (s, 3H, C-5 CH₃), 2.07–2.24 (m, 2H, CHCHH_ACH₃ + CHCHH_BCH₃, overlapped signals), 3.87–3.89 (m, 1H, SCH), 4.31–4.36 (m, 1H, CHCH₂CH₃), 6.79–6.91 (m, 2H, C_{3,5}-H Ar), 7.10–7.20 (m, 1H, C₄-H Ar), 9.80 (bs, 1H, NH exchangeable with D₂O). ESI-MS *m/z*: 353 (M + H)⁺. Anal. (C₁₈H₂₂F₂N₂OS) C, H, N.

2-(Cyclopentylthio)-6-(1-(2,6-difluorophenyl)propyl)-5-methylpyrimidin-4(3H)-one (3h). Title compound **3h** was obtained as a white solid (60%) starting from **2b** (1.00 g, 3.37 mmol) and bromocyclopentane (430 μ L, 3.71 mmol) according to the same procedure used for **3e**. Mp 195–197 °C (benzene/cyclohexane). ¹H NMR (300 MHz, CDCl₃) δ 0.89–0.94 (t, *J* = 7.2 Hz, 3H, CHCH₂CH₃), 1.63–1.75 (m, 6H, C_{3,4}-H₂ + C_{2,5}-H cyclopentane, overlapped signals), 1.95–2.24 (m, 4H, C_{2,5}-H cyclopentane + CHCHH_ACH₃ + CHCHH_BCH₃, overlapped signals), 2.05 (s, 3H, C-5 CH₃), 3.90–3.94 (m, 1H, SCH), 4.32–4.35 (m, 1H, CHCH₂CH₃), 6.80–6.86 (m, 2H, C_{3,5}-H Ar), 7.14–7.20 (m, 1H, C₄-H Ar), 12.70 (bs,

1H, NH exchangeable with D₂O). ESI-MS *m/z*: 365 (M + H)⁺. Anal. (C₁₉H₂₂F₂N₂O₅) C, H, N.

Biology. Cell Cultures. Human A375 melanoma (ATCC-CRL-1619) cells were seeded in six-well plates at a density of 1×10^4 to 5×10^4 cells/well and cultured in Dulbecco's modified Eagle medium (DMEM, Euroclone) with 10% (v/v) fetal calf serum, L-glutamine (2 mM), penicillin (100 IU/mL), and streptomycin (100 mg/mL) at 37 °C in a humidified 5% CO₂ atmosphere. After 5–6 h, when cells were adherent, RT inhibitors were dissolved in DMSO at the indicated concentrations, or the same volume of dimethylsulfoxide (DMSO, Aldrich; 0.005% final concentration) was added. Nevirapine and efavirenz were purified from commercially available Viramune (Boehringer-Ingelheim) and Sustiva (Bristol-Myers Squibb) as described.⁶² Compounds **2a,b** and **3a–h**, as well as the reference drugs nevirapine and efavirenz, were solubilized in DMSO. Fresh RT inhibitor-containing medium was changed every 48 h.

Proliferation Assays. To measure proliferation, cells were plated at an initial density of $(20–50) \times 10^3$ cells/35 mm diameter plate. After 48 or 96 h of culture, viable cells were scraped off and counted in a ZM Coulter counter (two countings per sample). Cell viability was also assessed using the trypan blue dye exclusion method in a Burkler chamber. The basal proliferation rate was estimated using the formula $[\text{cell } n(t)]/[\text{cell } n(t_0)]$, where the number of cells at t_0 is the number of seeded cells and the number of cells at time t is given by cell counts after 48 or 96 h of culture.

Apoptosis Analysis. For single-cell analysis of apoptotic cell death, A375 cells grown in culture dishes on sterile coverslips were stained with 4',6-diamidino-2-phenylindole (DAPI, Sigma) to visualize the nuclear morphology and with 3,3'-dihexyloxycarbocyanine iodide [DiOC6(3), Molecular Probes], a fluorescent probe for mitochondrial transmembrane potential. As a second assay, processed caspase-3 was detected using rabbit antiactive caspase-3 (ab13847, Abcam) followed by Cy3-conjugated donkey anti-rabbit secondary antibody (711-165-152, Jackson ImmunoResearch Laboratories) in fixed A375 cells samples counterstained with DAPI (data not shown). Cells were then analyzed under an epifluorescence Olympus AX70 microscope with a CCD camera (Photometrics) or Leica DMR with a CoolSnap (Photometrics).²⁴ Apoptosis was also assessed at the whole cell population level by biparametric FACS analysis of the nuclear DNA content (PI incorporation, linear scale) and of the cell granular density (side scatter analysis, SSC, logarithmic scale) or after incubation with annexin V-FITC (Immunological Sciences, IK-11120) and propidium iodide (PI, Sigma-Aldrich), as recommended by the suppliers. Cell samples were analyzed in a Coulter Epics XL cytofluorimeter (Beckman Coulter) equipped with EXPO 32 ADC software. At least 10 000 cells per sample were acquired.

Indirect Immunofluorescence and Confocal Microscopy. A375 cell preparations were fixed with 4% paraformaldehyde for 10 min and permeabilized in 0.2% Triton-X100 in phosphate buffered saline (PBS) for 5 min. Mouse monoclonal antibody α -tubulin (Molecular Probes, A-11126) was revealed by Alexa Fluor 488 conjugated secondary antibody (Molecular Probes, A-11001) or with horse anti-mouse Texas Red (Vector, TI-2000). Primary antibodies to human vimentin intermediate filaments were a generous gift from Genrich Tolstonog (Heinrich-Pette Institute für Experimentelle Virologie und Immunologie, Hamburg University, Germany) and were detected with FITC-conjugated secondary antibodies (Santa Cruz, sc-2090). Nuclei were stained either with 2 $\mu\text{g/mL}$ PI in the presence of 0.1 $\mu\text{g/mL}$ ribonuclease A or with 0.1 $\mu\text{g/mL}$ DAPI. Coverslips were mounted in Vectashield (Vector) and examined under an epifluorescence Olympus AX70 microscope with a CCD camera (Photometrics). For confocal analysis, samples were imaged under a confocal Leica TCS 4D microscope equipped with an argon/krypton laser. Confocal sections were taken at 0.5–1 μm intervals.

Tumor Xenografts and Treatment of Animals. Five-week-old athymic nude mice (Harlan, Italy) were inoculated subcutaneously with A375 melanoma cells (5×10^6) in 100 μL of PBS. Mice were intraperitoneally injected daily 5 days a week with efavirenz, **3g**, or isomer (–)-**3g'** (all at 20 mg/kg) using a 4 mg/mL stock in EtOH freshly diluted 1:5 with physiological solution. Controls were injected with 20% EtOH. Treatment started 1 week after tumor implant and was discontinued after 30 days. Tumor growth was monitored every other day by caliper measurement. Tumor volumes (V_T) were calculated using the following formula:⁶³

$$V_T = \text{length} \times \text{width} \times \text{height} \times 0.52$$

All animals were maintained in accordance with the European Union guidelines.

■ ASSOCIATED CONTENT

S Supporting Information. Elemental analysis results for compounds **3a–h** and additional biological data. This material is available free of charge via the Internet at <http://pubs.acs.org>.

■ AUTHOR INFORMATION

Corresponding Author

*For G.S.: phone, +39-089-96-9770; fax, +39-089-96-9602; e-mail, gsbardella@unisa.it. For A.M.: phone, +39-06-4991-3392; fax, +3906-49693268; e-mail, antonello.mai@uniroma1.it.

■ ACKNOWLEDGMENT

We acknowledge the skillful technical assistance of Enrico Cardarelli in the in vivo experiments with the murine models. This work was supported by grants from Università di Salerno, Italy (G.S.), COST Action TD09/05 Epigenetics (G.S. and A.M.), Fondazione Roma (A.M.), Ministero dell'Università e della Ricerca Scientifica e Tecnologica, PRIN 2008 (S.C. and P.L.), AIRC (P.L.), Ministero della Salute (Grants 7OCF/6 and Q5F, C.S.). C.M. was supported by a predoctoral fellowship from Università di Salerno, Italy.

■ ABBREVIATIONS USED

Alu, short interspersed element recognized by the Alu endonuclease, from *Arthrobacter luteus*; cDNA, complementary DNA; DAPI, 4',6-diamidino-2-phenylindole; DiOC6(3), 3,3'-dihexyloxycarbocyanine iodide; HERV, human endogenous retrovirus; hTERT, human telomerase reverse transcriptase; LINE-1, long interspersed element 1; LTR, long terminal repeat; NNRTI, non-nucleoside reverse transcriptase inhibitor; PBS, phosphate buffer saline; RT, reverse transcriptase; RNAi, RNA interference; SINE, short interspersed element; siRNA, small interfering RNA; SVA, SINE-VNTR-Alu; VNTR, variable number tandem repeat

■ REFERENCES

- (1) International Human Genome Sequencing Consortium.. Initial sequencing and analysis of the human genome. *Nature* **2001**, *409*, 860–921.
- (2) Cordaux, R.; Batzer, M. A. The impact of retrotransposons on human genome evolution. *Nat. Rev. Genet.* **2009**, *10*, 691–703.
- (3) Faulkner, G. J.; Kimura, Y.; Daub, C. O.; Wani, S.; Plessy, C.; Irvine, K. M.; Schroder, K.; Cloonan, N.; Steptoe, A. L.; Lassmann, T.; Waki, K.; Hornig, N.; Arakawa, T.; Takahashi, H.; Kawai, J.; Forrest, A. R. R.; Suzuki, H.; Hayashizaki, Y.; Hume, D. A.; Orlando, V.;

Grimmond, S. M.; Carninci, P. The regulated retrotransposon transcriptome of mammalian cells. *Nat. Genet.* **2009**, *41*, 563–571.

(4) Kazazian, H. H., Jr. Mobile elements: drivers of genome evolution. *Science* **2004**, *303*, 1626–1632.

(5) Goodier, J. L.; Kazazian, H. H., Jr. Retrotransposons revisited: the restraint and rehabilitation of parasites. *Cell* **2008**, *135*, 23–35.

(6) Hancks, D. C.; Kazazian, H. H., Jr. SVA retrotransposons: evolution and genetic instability. *Semin. Cancer Biol.* **2010**, *20*, 234–245.

(7) Mattick, J. S. A new paradigm for developmental biology. *J. Exp. Biol.* **2007**, *210*, 1526–1547.

(8) Taft, R. J.; Pheasant, M.; Mattick, J. S. The relationship between non-protein-coding DNA and eukaryotic complexity. *BioEssays* **2007**, *29*, 288–299.

(9) Doolittle, W. F.; Sapienza, C. Selfish genes, the phenotype paradigm and genome evolution. *Nature* **1980**, *284*, 601–603.

(10) Orgel, L. E.; Crick, F. H. Selfish DNA: the ultimate parasite. *Nature* **1980**, *284*, 604–607.

(11) Banerjee, S.; Thampan, R. V. Reverse transcriptase activity in bovine bone marrow: purification of a 66-kDa enzyme. *Biochim. Biophys. Acta, Protein Struct. Mol. Enzymol.* **2000**, *1480*, 1–5.

(12) Medstrand, P.; Blomberg, J. Characterization of novel reverse transcriptase encoding human endogenous retroviral sequences similar to type A and type B retroviruses: differential transcription in normal human tissues. *J. Virol.* **1993**, *67*, 6778–6787.

(13) Mwenda, J. M. Biochemical characterization of a reverse transcriptase activity associated with retroviral-like particles isolated from human placental villous tissue. *Cell. Mol. Biol.* **1993**, *39*, 317–328.

(14) Packer, A. I.; Manova, K.; Bachvarova, R. F. A discrete LINE-1 transcript in mouse blastocysts. *Dev. Biol. (Amsterdam, Neth.)* **1993**, *157*, 281–283.

(15) Poznanski, A. A.; Calarco, P. G. The expression of intracisternal A particle genes in the preimplantation mouse embryo. *Dev. Biol. (Amsterdam, Neth.)* **1991**, *143*, 271–281.

(16) Deragon, J. M.; Sinnett, D.; Labuda, D. Reverse transcriptase activity from human embryonal carcinoma cells NTera2D1. *EMBO J.* **1990**, *9*, 3363–3368.

(17) Friedlander, A.; Patarca, R. Endogenous proviruses. *Crit. Rev. Oncog.* **1999**, *10*, 129–59.

(18) Spadafora, C. Endogenous reverse transcriptase: a mediator of cell proliferation and differentiation. *Cytogenet. Genome Res.* **2004**, *105*, 346–350.

(19) Contreras-Galindo, R.; Kaplan, M. H.; Leissner, P.; Verjat, T.; Ferlenghi, I.; Bagnoli, F.; Giusti, F.; Dosik, M. H.; Hayes, D. F.; Gitlin, S. D.; Markovitz, D. M. Human endogenous retrovirus K (HML-2) elements in the plasma of people with lymphoma and breast cancer. *J. Virol.* **2008**, *82*, 9329–9336.

(20) Kurth, R.; Bannert, N. Beneficial and detrimental effects of human endogenous retroviruses. *Int. J. Cancer* **2010**, *126*, 306–314.

(21) di Marzo Veronese, F.; Copeland, T.; DeVico, A.; Rahman, R.; Oroszlan, S.; Gallo, R.; Sarngadharan, M. Characterization of highly immunogenic p66/p51 as the reverse transcriptase of HTLV-III/LAV. *Science* **1986**, *231*, 1289–1291.

(22) Ren, J.; Nichols, C.; Bird, L.; Chamberlain, P.; Weaver, K.; Short, S.; Stuart, D. I.; Stammers, D. K. Structural mechanisms of drug resistance for mutations at codons 181 and 188 in HIV-1 reverse transcriptase and the improved resilience of second generation non-nucleoside inhibitors. *J. Mol. Biol.* **2001**, *312*, 795–805.

(23) Mangiacasale, R.; Pittoggi, C.; Sciamanna, I.; Careddu, A.; Mattei, E.; Lorenzini, R.; Travaglini, L.; Landriscina, M.; Barone, C.; Nervi, C.; Lavia, P.; Spadafora, C. Exposure of normal and transformed cells to nevirapine, a reverse transcriptase inhibitor, reduces cell growth and promotes differentiation. *Oncogene* **2003**, *22*, 2750–2761.

(24) Sciamanna, I.; Landriscina, M.; Pittoggi, C.; Quirino, M.; Mearelli, C.; Beraldi, R.; Mattei, E.; Serafino, A.; Cassano, A.; Sinibaldi-Vallebona, P.; Garaci, E.; Barone, C.; Spadafora, C. Inhibition of endogenous reverse transcriptase antagonizes human tumor growth. *Oncogene* **2005**, *24*, 3923–3931.

(25) Bartolini, S.; Mai, A.; Artico, M.; Paesano, N.; Rotili, D.; Spadafora, C.; Sbardella, G. 6-[1-(2,6-Difluorophenyl)ethyl]pyrimidinones antagonize cell proliferation and induce cell differentiation by inhibiting (a nonoligomeric) endogenous reverse transcriptase. *J. Med. Chem.* **2005**, *48*, 6776–6778.

(26) Sbardella, G.; Bartolini, S.; Castellano, S.; Artico, M.; Paesano, N.; Rotili, D.; Spadafora, C.; Mai, A. 6-Alkylthio-4-[1-(2,6-difluorophenyl)alkyl]-1H-[1,3,5]triazin-2-ones (ADATs): novel regulators of cell differentiation and proliferation. *ChemMedChem* **2006**, *1*, 1073–1080.

(27) Sinibaldi-Vallebona, P.; Lavia, P.; Garaci, E.; Spadafora, C. A role for endogenous reverse transcriptase in tumorigenesis and as a target in differentiating cancer therapy. *Genes, Chromosomes Cancer* **2006**, *45*, 1–10.

(28) Jones, R. B.; Garrison, K. E.; Wong, J. C.; Duan, E. H.; Nixon, D. F.; Ostrowski, M. A. Nucleoside analogue reverse transcriptase inhibitors differentially inhibit human LINE-1 retrotransposition. *PLoS One* **2008**, *3*, e1547.

(29) Carlini, F.; Ridolfi, B.; Molinari, A.; Parisi, C.; Bozzuto, G.; Toccaceli, L.; Formisano, G.; De Orsi, D.; Paradisi, S.; Grober, O. M. V.; Ravo, M.; Weisz, A.; Arcieri, R.; Vella, S.; Gaudi, S. The reverse transcription inhibitor abacavir shows anticancer activity in prostate cancer cell lines. *PLoS One* **2010**, *5*, e14221.

(30) Spadafora, C. A reverse transcriptase-dependent mechanism plays central roles in fundamental biological processes. *Syst. Biol. Reprod. Med.* **2008**, *54*, 11–21.

(31) Landriscina, M.; Spadafora, C.; Cignarelli, M.; Barone, C. Antitumor activity of non-nucleosidic reverse transcriptase inhibitors. *Curr. Pharm. Des.* **2007**, *13*, 737–747.

(32) Artico, M.; Massa, S.; Mai, A.; Marongiu, M. E.; Piras, G.; Tramontano, E.; Lacolla, P. 3,4-Dihydro-2-alkoxy-6-benzyl-4-oxopyrimidines (DABOs): a new class of specific inhibitors of human immunodeficiency-virus type-1. *Antiviral Chem. Chemother.* **1993**, *4*, 361–368.

(33) Massa, S.; Mai, A.; Artico, M.; Sbardella, G.; Tramontano, E.; Loi, A. G.; Scano, P.; La Colla, P. Synthesis and antiviral activity of new 3,4-dihydro-2-alkoxy-6-benzyl-4-oxopyrimidines (DABOs), specific inhibitors of human immunodeficiency virus type-1. *Antiviral Chem. Chemother.* **1995**, *6*, 1–8.

(34) Mai, A.; Artico, M.; Sbardella, G.; Massa, S.; Loi, A. G.; Tramontano, E.; Scano, P.; La Colla, P. Preparation and anti-HIV-1 activity of thio analogues of dichydroalkoxybenzylloxopyrimidines. *J. Med. Chem.* **1995**, *38*, 3258–3263.

(35) Mai, A.; Artico, M.; Sbardella, G.; Quartarone, S.; Massa, S.; Loi, A. G.; De Montis, A.; Scintu, F.; Putzolu, M.; La Colla, P. Dihydro-(alkylthio)(naphthylmethyl)oxopyrimidines: novel non-nucleoside reverse transcriptase inhibitors of the S-DABO series. *J. Med. Chem.* **1997**, *40*, 1447–1454.

(36) Mai, A.; Artico, M.; Sbardella, G.; Massa, S.; Novellino, E.; Greco, G.; Loi, A. G.; Tramontano, E.; Marongiu, M. E.; La Colla, P. 5-Alkyl-2-(alkylthio)-6-(2,6-dihalophenylmethyl)-3,4-dihydropyrimidin-4(3H)-ones: novel potent and selective dihydro-alkoxy-benzyl-oxopyrimidine derivatives. *J. Med. Chem.* **1999**, *42*, 619–627.

(37) Sbardella, G.; Mai, A.; Artico, M.; Massa, S.; Marceddu, T.; Vargiu, L.; Marongiu, M. E.; La Colla, P. Does the 2-methylthiomethyl substituent really confer high anti-HIV-1 activity to S-DABOs? *Med. Chem. Res.* **2000**, *10*, 30–39.

(38) Mai, A.; Sbardella, G.; Artico, M.; Ragno, R.; Massa, S.; Novellino, E.; Greco, G.; Lavecchia, A.; Musiu, C.; La Colla, M.; Murgioni, C.; La Colla, P.; Loddo, R. Structure-based design, synthesis, and biological evaluation of conformationally restricted novel 2-alkylthio-6-[1-(2,6-difluorophenyl)alkyl]-3,4-dihydro-5-alkylpyrimidin-4(3H)-ones as non-nucleoside inhibitors of HIV-1 reverse transcriptase. *J. Med. Chem.* **2001**, *44*, 2544–2554.

(39) Sbardella, G.; Mai, A.; Artico, M.; Chimenti, P.; Massa, S.; Loddo, R.; Marongiu, M. E.; La Colla, P.; Pani, A. Structure–activity relationship studies on new DABOs: effect of substitutions at pyrimidine C-5 and C-6 positions on anti-HIV-1 activity. *Antiviral Chem. Chemother.* **2001**, *12*, 37–50.

- (40) Ragno, R.; Mai, A.; Sbardella, G.; Artico, M.; Massa, S.; Musiu, C.; Mura, M.; Marturana, F.; Cadeddu, A.; La Colla, P. Computer-aided design, synthesis, and anti-HIV-1 activity in vitro of 2-alkylamino-6-[1-(2,6-difluorophenyl)alkyl]-3,4-dihydro-5-alkylpyrimidin-4(3H)-ones as novel potent non-nucleoside reverse transcriptase inhibitors, also active against the Y181C variant. *J. Med. Chem.* **2004**, *47*, 928–934.
- (41) Mai, A.; Artico, M.; Ragno, R.; Sbardella, G.; Massa, S.; Musiu, C.; Mura, M.; Marturana, F.; Cadeddu, A.; Maga, G.; Colla, P. L. 5-Alkyl-2-alkylamino-6-(2,6-difluorophenylalkyl)-3,4-dihydropyrimidin-4(3H)-ones, a new series of potent, broad-spectrum non-nucleoside reverse transcriptase inhibitors belonging to the DABO family. *Bioorg. Med. Chem.* **2005**, *13*, 2065–2077.
- (42) Cancio, R.; Mai, A.; Rotili, D.; Artico, M.; Sbardella, G.; Clotet-Codina, I.; Esté, J. A.; Crespan, E.; Zanolli, S.; Hübscher, U.; Spadari, S.; Maga, G. Slow-, tight-binding HIV-1 reverse transcriptase non-nucleoside inhibitors highly active against drug-resistant mutants. *ChemMedChem* **2007**, *2*, 445–448.
- (43) Mai, A.; Artico, M.; Rotili, D.; Tarantino, D.; Clotet-Codina, I.; Armand-Ugón, M.; Ragno, R.; Simeoni, S.; Sbardella, G.; Nawrozkij, M. B.; Samuele, A.; Maga, G.; Esté, J. A. Synthesis and biological properties of novel 2-aminopyrimidin-4(3H)-ones highly potent against HIV-1 mutant strains. *J. Med. Chem.* **2007**, *50*, 5412–5424.
- (44) Gomez, D.; Lemarteleur, T.; Lacroix, L.; Mailliet, P.; Mergny, J.-L.; Riou, J.-F. Telomerase downregulation induced by the G-quadruplex ligand 12459 in A549 cells is mediated by hTERT RNA alternative splicing. *Nucleic Acids Res.* **2004**, *32*, 371–379.
- (45) Mugnaini, C.; Alongi, M.; Togninelli, A.; Gevariya, H.; Brizzi, A.; Manetti, F.; Bernardini, C.; Angeli, L.; Tafi, A.; Bellucci, L.; Corelli, F.; Massa, S.; Maga, G.; Samuele, A.; Facchini, M.; Clotet-Codina, I.; Armand-Ugón, M.; Esté, J. A.; Botta, M. Dihydro-alkylthio-benzyl-oxopyrimidines as inhibitors of reverse transcriptase: synthesis and rationalization of the biological data on both wild-type enzyme and relevant clinical mutants. *J. Med. Chem.* **2007**, *50*, 6580–6595.
- (46) Oricchio, E.; Sciamanna, I.; Beraldi, R.; Tolstonog, G. V.; Schumann, G. G.; Spadafora, C. Distinct roles for LINE-1 and HERV-K retroelements in cell proliferation, differentiation and tumor progression. *Oncogene* **2007**, *26*, 4226–4233.
- (47) Sauane, M.; Gopalkrishnan, R. V.; Sarkar, D.; Su, Z.-Z.; Lebedeva, I. V.; Dent, P.; Pestka, S.; Fisher, P. B. MDA-7/IL-24: novel cancer growth suppressing and apoptosis inducing cytokine. *Cytokine Growth Factor Rev.* **2003**, *14*, 35–51.
- (48) Cirilli, R.; Ferretti, R.; Gallinella, B.; Torre, F. L.; Mai, A.; Rotili, D. Analytical and semipreparative high performance liquid chromatography separation of stereoisomers of novel 3,4-dihydropyrimidin-4(3H)-one derivatives on the immobilised amylose-based Chiralpak IA chiral stationary phase. *J. Sep. Sci.* **2006**, *29*, 1399–1406.
- (49) Cirilli, R.; Ferretti, R.; La Torre, F.; Borioni, A.; Fares, V.; Camalli, M.; Faggi, C.; Rotili, D.; Mai, A. Chiral HPLC separation and absolute configuration of novel S-DABO derivatives. *Chirality* **2009**, *21*, 604–612.
- (50) Kepp, O.; Galluzzi, L.; Lipinski, M.; Yuan, J.; Kroemer, G. Cell death assays for drug discovery. *Nat. Rev. Drug Discovery* **2011**, *10*, 221–237.
- (51) Sinibaldi-Vallebona, P.; Matteucci, C.; Spadafora, C. Retrotransposon-encoded reverse transcriptase in the genesis, progression and cellular plasticity of human cancer. *Cancers* **2011**, *3*, 1141–1157.
- (52) Rossi, A.; Russo, G.; Puca, A.; Montagna, R. L.; Caputo, M.; Mattioli, E.; Lopez, M.; Giordano, A.; Pentimalli, F. The antiretroviral nucleoside analogue abacavir reduces cell growth and promotes differentiation of human medulloblastoma cells. *Int. J. Cancer* **2009**, *125*, 235–243.
- (53) Landriscina, M.; Bagalà, C.; Piscazzi, A.; Schinzari, G.; Quirino, M.; Fabiano, A.; Bianchetti, S.; Cassano, A.; Sica, G.; Barone, C. Nevirapine restores androgen signaling in hormone-refractory human prostate carcinoma cells both in vitro and in vivo. *Prostate* **2009**, *69*, 744–754.
- (54) Chow, W. A.; Jiang, C.; Guan, M. Anti-HIV drugs for cancer therapeutics: back to the future? *Lancet Oncol.* **2009**, *10*, 61–71.
- (55) Landriscina, M.; Altamura, S. A.; Roca, L.; Gigante, M.; Piscazzi, A.; Cavalcanti, E.; Costantino, E.; Barone, C.; Cignarelli, M.; Gesualdo, L.; Ranieri, E. Reverse transcriptase inhibitors induce cell differentiation and enhance the immunogenic phenotype in human renal clear-cell carcinoma. *Int. J. Cancer* **2008**, *122*, 2842–2850.
- (56) Humer, J.; Ferko, B.; Waltenberger, A.; Rapberger, R.; Pehamberger, H.; Muster, T. Azidothymidine inhibits melanoma cell growth in vitro and in vivo. *Melanoma Res.* **2008**, *18*, 314–321.
- (57) Golan, M.; Hizi, A.; Resau, J. H.; Yaal-Hahoshen, N.; Reichman, H.; Keydar, I.; Tsarfaty, I. Human endogenous retrovirus (HERV-K) reverse transcriptase as a breast cancer prognostic marker. *Neoplasia (Ann Arbor, MI, U. S.)* **2008**, *10*, 521–533.
- (58) Landriscina, M.; Fabiano, A.; Altamura, S.; Bagala, C.; Piscazzi, A.; Cassano, A.; Spadafora, C.; Giorgino, F.; Barone, C.; Cignarelli, M. Reverse transcriptase inhibitors down-regulate cell proliferation in vitro and in vivo and restore thyrotropin signaling and iodine uptake in human thyroid anaplastic carcinoma. *J. Clin. Endocrinol. Metab.* **2005**, *90*, 5663–5671.
- (59) Damm, K.; Hemmann, U.; Garin-Chesa, P.; Huel, N.; Kauffmann, I.; Pripke, H.; Niestroj, C.; Daiber, C.; Enenkel, B.; Guilliard, B.; Lauritsch, I.; Muller, E.; Pascolo, E.; Sauter, G.; Pantic, M.; Martens, U. M.; Wenz, C.; Lingner, J.; Kraut, N.; Rettig, W. J.; Schnapp, A. A highly selective telomerase inhibitor limiting human cancer cell proliferation. *EMBO J.* **2001**, *20*, 6958–6968.
- (60) Blasco, M. A.; Lee, H.-W.; Hande, M. P.; Samper, E.; Lansdorp, P. M.; DePinho, R. A.; Greider, C. W. Telomere shortening and tumor formation by mouse cells lacking telomerase RNA. *Cell* **1997**, *91*, 25–34.
- (61) Methylene protons are anisochronous because of the effect of the adjacent chiral center: Nair, P. M.; Roberts, J. D. Nuclear magnetic resonance spectra. Hindered rotation and molecular asymmetry. *J. Am. Chem. Soc.* **1957**, *79*, 4565–4566.
- (62) Pittoggi, C.; Sciamanna, I.; Mattei, E.; Beraldi, R.; Lobascio, A. M.; Mai, A.; Quaglia, M. G.; Lorenzini, R.; Spadafora, C. Role of endogenous reverse transcriptase in murine early embryo development. *Mol. Reprod. Dev.* **2003**, *66*, 225–236.
- (63) Umekita, Y.; Hiipakka, R. A.; Kokontis, J. M.; Liao, S. Human prostate tumor growth in athymic mice: inhibition by androgens and stimulation by finasteride. *Proc. Natl. Acad. Sci. U.S.A.* **1996**, *93*, 11802–11807.